Correlation between Structures and Ionic Conductivities of Na$_2$Ln$_2$Ti$_3$O$_{10}$ (Ln=La, Nd, Sm, and Gd)

Kileung Park and Song-Ho Byeon*

Department of Chemistry, College of Natural Sciences, Kyung Hee University, Kyung-Ki 449-701, Korea
Received October 16, 1995

The variations of the structural detail of layered perovskite-type oxides, Na$_2$Ln$_2$Ti$_3$O$_{10}$ (Ln=La, Nd, Sm, Gd), have been refined by Rietveld analyses of their powder X-ray diffraction data. Although the c-axis strongly decreases from Ln=La to Nd, Sm, or Gd, the length of Na-O bond along the c-axis that is regarded as the sodium layer spacing is not dependent on the unit cell parameter. Such a behavior is explained by the fact that Na-O bond is in competition with Ti-O one of the perovskite slab. Increased covalency of this Ti-O bond by the lattice contraction leads to weakening of the attaching strength of Na ion. This picture is consistent with the experimental observation that Na ion conductivity of Na$_2$Ln$_2$Ti$_3$O$_{10}$ increases from Ln=La to Nd, Sm, or Gd despite strong contraction of the unit cell volume.

Introduction

A number of layered perovskite type oxides A'$_2$[A$_{n-1}$B$_n$ O$_{3n+1}$], which are one of Ruddlesden-Popper family, are known.[1~3] They consist of perovskite slabs with multiple stacked BO$_6$ octahedra which are separated by double layer of A' ions occupying the sodium position of rock-salt type. High ionic conductivity of the similar layered compounds with particularly Ti and/or Nb result in alkali ion exchange reactions in molten salts including proton exchange in aqueous acid, the intercalation reactions, and the interlayer chemistry between perovskite slabs.[4~7]

A series of layered perovskite with general formular A$_2$ [Ln$_2$Ti$_3$O$_{10}$](A=Na, K, Rb; Ln=La, Nd, Sm, Gd, Dy) has been synthesized by many authors.[8,9] During our work, the crystal structure of Na$_2$La$_2$Ti$_3$O$_{10}$ and Na$_2$Nd$_2$Ti$_3$O$_{10}$ have been determined.[10,11] Low ionic conductivity of Na$_2$La$_2$Ti$_3$O$_{10}$ compared with those of niobium analogues, NaLaNb$_2$O$_7$ and NaCa$_2$-NaNb$_4$O$_{13}$,[12] was discussed on the basis of the difference of coordination around sodium ion. Comparing K$_2$La$_2$Ti$_3$O$_{10}$ and Na$_2$La$_2$Ti$_3$O$_{10}$, the former allows spontaneous water intercalation between the perovskite slabs while the latter is not reactive with water. Variable Brφnsted acidities of proton exchanged similar layered perovskites are explained and controlled by the attaching strength of proton along the direction perpendicular to the layer between the perovskite slabs.[13]

If we consider three-dimensional perovskite type oxides with vacant sites available for the mobile ions, their ionic conductivities are strongly influenced by the size of unit cell volume. The conductivity generally decreases with increasing lattice contraction. Since their conduction channel is three-dimensionally linked, the lattice contraction resulting from the replacement of the larger ion by the smaller one leads to a decrease of the bottleneck size. Similarly, the application of external hydrostatic pressure also gives same effect. In such a criterion, it is agreeable that lithium ion conductivities in Ln$_{0.5}$Li$_{0.5}$TiO$_3$ are lowered with decreasing the radii of lanthanide ions (from Ln=La to Pr, Nd, and Sm).[14] On the other hand, the increase of sodium content in [(La$_{0.5}$Li$_{0.5}$)$_{1-x}$ (La$_{0.5}$Na$_{0.5}$)$_x$]TiO$_3$ lowers the ionic conductivity in spite of the lattice expansion. This indicates that sodium ion does not contribute to the ionic conductivity but decreases the availa-

ble space for the migration of the lithium ion.[15]

If sodium ions do not migrate through the perovskite lattice as in La$_{0.5}$Na$_{0.5}$TiO$_3$, sodium ion conductivity observed in Na$_2$La$_2$Ti$_3$O$_{10}$ containing central LaTiO$_3$ slab would be induced by the migration of sodium ion only through the sodium layer. The ionic conductivity will not be influenced by the contraction of perovskite slab giving rise to the decrease of unit cell volume. However, we observed considerable change of sodium ion conductivity when La is replaced by Nd, Sm, or Gd in Na$_2$Ln$_2$Ti$_3$O$_{10}$. In this work, the crystal structures of Na$_2$Ln$_2$Ti$_3$O$_{10}$(Ln=La, Nd, Sm, and Gd) series have been refined by Rietveld analysis of their powder X-ray diffraction data to compare the lengths of Na-O and Ti-O bond perpendicular to the c-axis. On the basis of structural details, the variation of sodium ion conductivity are correlated to that of the covalency of Na-O bond.

Experimental

At first, the preparations of title compounds were tried by the ion-exchange of K$_2$Ln$_2$Ti$_3$O$_{10}$(Ln=La, Nd, Sm, and Gd) in molten NaNO$_3$ according to the literature.[9] Since the products were not well crystallized and contained considerable amounts of unidentifiable impurity phases, however, Na$_2$Ln$_2$ Ti$_3$O$_{10}$(Ln=La, Nd, Sm, and Gd) discussed in this report were prepared by conventional solid state reactions. The stoichiometric amounts of Ln$_2$O$_3$ and TiO$_2$ (anatase) and 20% excess of Na$_2$CO$_3$ were mixed, slowly heated up to 800 ℃ (1 ℃/min.), and kept constant for 12 hours in air. Ln$_2$O$_3$ was preheated at 900 ℃ for 12 hours, cooled to room temperature, and directly weighed. The resulting powder was ground after the addition of 20% excess of Na$_2$CO$_3$, heated at 1050 ℃ for 2 days with two intermittent grindings, and cooled in the furnace. 20% excess of Na$_2$CO$_3$ was added on every grinding to compensate the loss of volatile sodium component. After the reaction, the products were washed with distilled water and dried at 110 ℃. For the specimens to measure ionic conductivity, the well dried products were pressed into the pellets and heated at 1100 ℃ for 5 hours.

The sodium contents in the final products were determined by inductively coupled plasma (ICP) method using BAIRD ICP 2070 instrument. The obtained molar ratios of

Structure and Na Conductivity of Na$_2$Ln$_2$Ti$_3$O$_{10}$

Bull. Korean Chem. Soc. 1996, Vol. 17, No. 2 169

Table 1. Sodium contents in Na$_2$Ln$_2$Ti$_3$O$_{10}$ determined by ICP

compounds	molar ratio of sodium per formular
Na$_2$La$_2$Ti$_3$O$_{10}$	1.99(1)
Na$_2$Nd$_2$Ti$_3$O$_{10}$	1.98(1)
Na$_2$Sm$_2$Ti$_3$O$_{10}$	1.99(2)
Na$_2$Gd$_2$Ti$_3$O$_{10}$	1.99(1)

sodium per formular unit have confirmed the stoichiometric formation of Na$_2$Ln$_2$Ti$_3$O$_{10}$ within experimental errors (Table 1).

The thermogravimetric analysis (TGA) and differential thermal analysis (DTA) were carried out from room temperature to 1500 K (5 K/min heating rate) under the air using TG/DTA 320 Seico Instruments Inc.

Powder X-ray diffraction data for Rietveld refinements were recorded on a rotating anode installed M18XHF MAC Science diffractometer using Cu Kα radiation monochromatized by the curved graphite. The data were collected with a step-scan procedure in the range 2θ=20° to 120° with counts for a second at 0.02° intervals. The fitting of reflection positions and intensities were carried out using Rietveld analysis program RIETAN (Macintosh version).[16]

Sodium ion conductivities of Na$_2$Ln$_2$Ti$_3$O$_{10}$ were measured on a Au pasted pellet by a complex impedance technique between 5 Hz and 13 MHz using a HP4192A impedance analyser in the temperature range of 300-1000 K.

Rerults and Discussion

Structure. The crystal structure of Na$_2$Ln$_2$Ti$_3$O$_{10}$(Ln= La, Nd, Sm, and Gd) were refined using initial atomic positions (space group I4/mmm) proposed by Ruddlesden and Popper.[1] Such refinements with the correction of the preferred orientation factor[17] gave relatively good fit with agreeable reliability factors as shown in Table 2. The observed, calculated, and difference profiles for one (Na$_2$La$_2$Ti$_3$O$_{10}$) of title compounds are plotted in Figure 1 and the refined structure parameters are listed in Table 3. In this table, very large isotropic thermal parameters for oxygen atoms are observed. As indicated by others,[10,11] the formation of NaLnTiO$_4$ or Na$_{0.5}$Ln$_{0.5}$TiO$_3$ as impurity phases would result in highly scattered isotropic thermal parameters. Indeed we have observed small
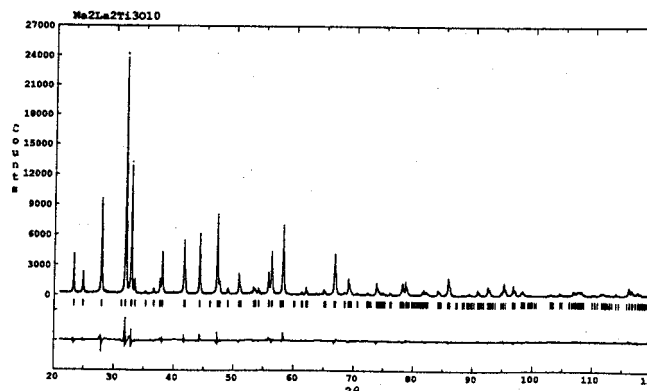
Figure 1. Calculated (solid line), experimental (dots), and difference (solid line on the bottom) X-ray powder diffraction pattern of Na$_2$La$_2$Ti$_3$O$_{10}$.

impurity NaLnTiO$_4$ phases in corresponding X-ray diffraction patterns, whose content strongly increased on heating at 950 °C for long time during preparation. The intensity data of these impurity peaks were excluded on refinements.

The selected bond lengths and bond angles are listed in Table 4 and the idealized perspective view of the unit cell is shown in Figure 2. The crystal lattice consists of slabs containing triple perovskite-like layers stacked along [001] direction which are separated by the rock-salt (NaO) type sodium bilayers. The Ti atoms are displaced out of TiO$_2$ plane toward the NaO double layers, leading to a considerable distortion of TiO$_2$ layers. There are large differences (~ 0.6 Å) in length between Ti(2)-O(1) and Ti(2)-O(3) bonds along the c-axis. The Ti(2)-O(3) distances (1.63 Å-1.72 Å) in strongly distorted Ti(2)O$_6$ octahedron are quite short compared with those in common perovskite type oxides. Very short Ti-O bond with double bond character was observed in some molecular compounds such as TiOCl$_2$ and TiOCl$_2$·2 POCl$_3$(18) and Bi$_4$Ti$_3$O$_{12}$.[19] But such a short distance in perovskite-type oxide may be exceptional. High ionic character of competing Na-O(3) bond would be consequently expected. Moreover, a decreasing trend of Ti(2)-O(3) bond length from Ln=La to Nd, Sm, and Gd plays important role on the ionic conductivity as we will discuss in the next section. The strong distortion of the Ti(2)O$_6$ octahedron is accompanied by the decrease of O(1)-Ln-O(1) bond angle but the Ti(1)O$_6$ units belonging to the central layer of the perovskite slab

Table 2. Crystallographic data for Na$_2$Ln$_2$Ti$_3$O$_{10}$(Ln=La, Nd, Sm, and Gd)

	Na$_2$La$_2$Ti$_3$O$_{10}$	Na$_2$Nd$_2$Ti$_3$O$_{10}$	Na$_2$Sm$_2$Ti$_3$O$_{10}$	Na$_2$Gd$_2$Ti$_3$O$_{10}$
Space group	I4/mmm	I4/mmm	I4/mmm	I4/mmm
a (Å)	3.83608(5)	3.8168(1)	3.8031(1)	3.7872(1)
c (Å)	28.5383(4)	28.2816(8)	28.2337(9)	28.2784(9)
V (cm³)	419.96	412.02	408.35	405.60
ρ (g/cm³)	4.96	5.14	5.29	5.44
Bragg (R_I, %)	3.93	4.70	6.60	4.07
Weighted profile (R_{WP}, %)	10.52	13.43	15.86	11.85
Profile (R_P, %)	7.92	9.79	10.66	8.96
Expected (R_E, %)	4.53	4.65	5.02	4.86

Table 3. Positional parameters for $Na_2Ln_2Ti_3O_{10}$(Ln=La, Nd, Sm, and Gd)

	$Na_2La_2Ti_3O_{10}$	$Na_2Nd_2Ti_3O_{10}$	$Na_2Sm_2Ti_3O_{10}$	$Na_2Gd_2Ti_3O_{10}$
Ln	La	Nd	Sm	Gd
x	0.0	0.0	0.0	0.0
y	0.0	0.0	0.0	0.0
z	0.4245(1)	0.4246(3)	0.4244(4)	0.4245(3)
B ($\AA^2$)	0.7(1)	0.9(2)	1.4(2)	2.2(2)
Na				
x	0.0	0.0	0.0	0.0
y	0.0	0.0	0.0	0.0
z	0.2901(8)	0.290(1)	0.291(2)	0.290(1)
B ($\AA^2$)	0.3(4)	0.2(8)	0.9(9)	1.0(9)
Ti(1)				
x	0.0	0.0	0.0	0.0
y	0.0	0.0	0.0	0.0
z	0.0	0.0	0.0	0.0
B ($\AA^2$)	0.6(3)	0.8(6)	0.9(8)	1.4(6)
Ti(2)				
x	0.0	0.0	0.0	0.0
y	0.0	0.0	0.0	0.0
z	0.1490(3)	0.1478(5)	0.1474(4)	0.1483(4)
B ($\AA^2$)	0.6	0.8	0.9	1.4
O(1)				
x	0.0	0.0	0.0	0.0
y	0.0	0.0	0.0	0.0
z	0.067(1)	0.068(3)	0.071(4)	0.067(3)
B ($\AA^2$)	1.1(8)	5(2)	5(2)	4(2)
O(2)				
x	0.0	0.0	0.0	0.0
y	0.5	0.5	0.5	0.5
z	0.0	0.0	0.0	0.0
B ($\AA^2$)	6(2)	5(2)	4(3)	5(3)
O(3)				
x	0.0	0.0	0.0	0.0
y	0.0	0.0	0.0	0.0
z	0.209(1)	0.207(2)	0.205(3)	0.207(3)
B ($\AA^2$)	0.8(8)	2(2)	3(2)	5(2)
O(4)				
x	0.0	0.0	0.0	0.0
y	0.5	0.5	0.5	0.5
z	0.136(1)	0.131(2)	0.131(2)	0.132(2)
B ($\AA^2$)	0.8(5)	0.8(8)	1.3(9)	3.2(9)

Table 4. Selected bond lengths ($\AA$) and bond angles (°) for $Na_2Ln_2Ti_3O_{10}$

	Ln=La	Nd	Sm	Gd
bond lengths				
Ti(1)-O(1) (X 2)	1.90(4)	1.91(8)	2.00(9)	1.88(8)
Ti(1)-O(2) (X 4)	1.9180(1)	1.9084(1)	1.9015(1)	1.8936(1)
Ti(2)-O(1) (X 1)	2.35(4)	2.27(9)	2.16(9)	2.31(9)
Ti(2)-O(3) (X 1)	1.72(4)	1.68(6)	1.63(8)	1.67(7)
Ti(2)-O(4) (X 4)	1.955(6)	1.97(1)	1.96(1)	1.95(1)
Na-O(3) (X 1)	2.31(5)	2.33(8)	2.42(9)	2.35(8)
(X 4)	2.7126(3)	2.701(3)	2.692(3)	2.679(2)
Ln-O(1) (X 4)	2.724(4)	2.708(7)	2.693(5)	2.690(8)
bond angles				
O(4)-Ti(2)-O(4)	158.1(5)	152.1(6)	152.7(6)	152.7(5)
O(3)-Na-O(3)	178.9(2)	176.4(4)	175.2(5)	176.4(4)
O(1)-Ln-O(1)	169.8(3)	171.1(5)	174.5(6)	169.8(6)
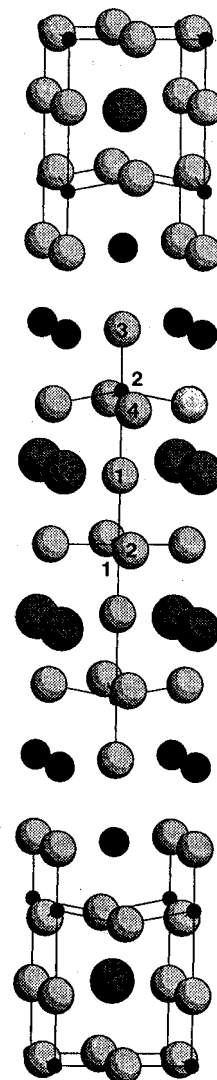
Figure 2. Perspective view of the structure for $Na_2Ln_2Ti_3O_{10}$. Only Ti-O bonds are described by lines. (Ln=shaded large spheres, Na=black large spheres, Ti=black small spheres, and O =white spheres).
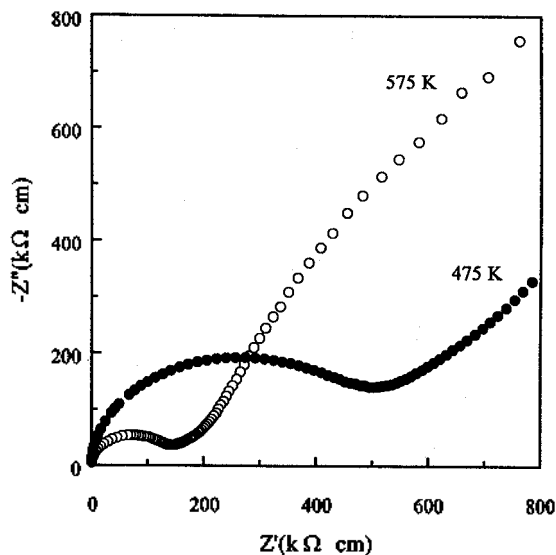
have nearly pure octahedral symmetry.

Ionic conductivity. As illustrated in Figure 3, the complex impedance plane plots of imaginary part Z'' against the real part Z' show a semi-circles and a spike. The ionic conductivity was obtained using the resistance values determined from the intersection of the semi-circle with the Z' axis. The logarithms of ionic conductivities of $Na_2Ln_2Ti_3O_{10}$(Ln= La, Nd, Sm, and Gd) as a function of reciprocal temperature are plotted in Figure 4. Although Toda *et al.* have observed a sharp drop of ionic conductivity for $Na_2La_2Ti_3O_{10}$ at around 575 ℃,[10] we could not observe such a behavior after even two cycles of heating and cooling between 300-726 ℃. In
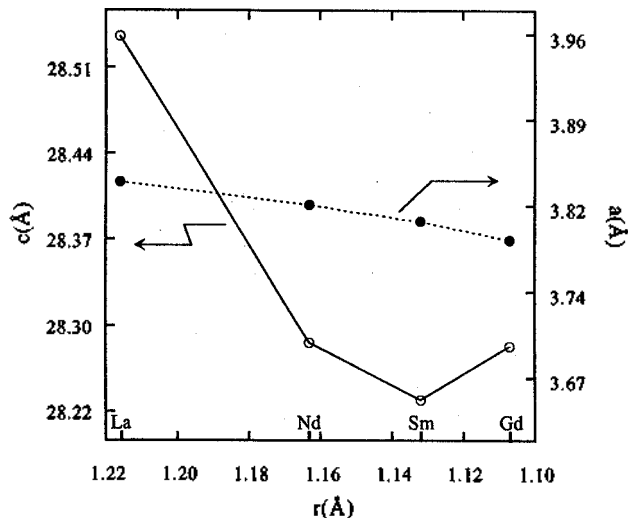
Figure 3. Complex impedance plane plots at 475 and 575 K for Na₂Sm₂Ti₃O₁₀.

Figure 5. Variations of the lattice parameters of Na₂Ln₂Ti₃O₁₀ (Ln = La, Nd, Sm, and Gd) as a function of the radii of lanthanide ions.

Figure 4. Plots of log σ *vs* 1/T for Na₂Ln₂Ti₃O₁₀(Ln = La, Nd, Sm, and Gd). The activation energies calculated from corresponding slopes are indicated in parentheses.
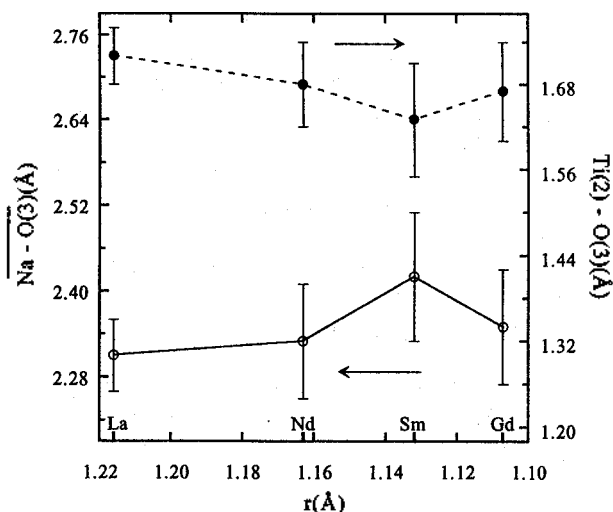
Figure 6. Variations of the Na-O(3) and Ti(2)-O(3) bond lengths in Na₂Ln₂Ti₃O₁₀(Ln = La, Nd, Sm, and Gd) as a function of the radii of lanthanide ions.

fact, the thermogravimetric and differential thermal analyses for Na₂Ln₂Ti₃O₁₀ did not show any evidence of decomposition up to 950 ℃. They were slowly decomposed into probably La₂/₃TiO₃ defective perovskite or Ln₂Ti₂O₇ (Ln = Nd, Sm, and Gd) pyrochlores at higher temperature.[9] Variation of the unit cell parameters is shown in Figure 5, where the *a*-parameter decreases linearly with decreasing the size of lanthanide ion and there is even strong decrease in the *c*-parameter. From this figure, it is intuitively expected that the higher lattice contraction for Ln = Nd, Sm, or Gd phases than La one would result in the lower ionic conductivity. It is interesting, however, that the ionic conductivity considerably increases from Ln = La to Nd, Sm, Gd phase with smaller unit cell volume. Na₂Sm₂Ti₃O₁₀ and Na₂Gd₂Ti₃O₁₀ show the conductivities comparable with the niobium compounds, NaLaNb₂O₇ and Na₂Ca₂

NaNb₄O₁₃.[12] In addition, an increase of the ionic conductivity is accompanied by a decrease of the activation energy. To understand such a trend, it may be helpful to compare the variation of the unit cell parameters with that of sodium layer spacing. Figure 6 shows the changes of Na-O(3) able to be regarded as sodium layer spacing and Ti(2)-O(3) distances in La₂Ln₂Ti₃O₁₀. The strong decrease of the *c*-parameter is observed when La ion is replaced by smaller Nd, Sm, or Gd as shown in Figure 5 whereas Na-O(3) distance shows reversely increasing trend. This behavior indicates that the decrease of the *c*-parameter results from the contraction of the perovskite slabs only, the variation of the sodium layer spacing not being explained in terms of that of the *c*-parameter. In this respect, it is necessary to consider the characteristic feature of layered perovskite structure. As shown in Figure 2, the Na-O(3) bond is in competition with the Ti

(2)-O(3) one whose covalency is strongly influenced by the contraction or expansion of perovskite slab. If the perovskite slabs are contracted by the decreases of the unit cell parameters, the increased covalency of Ti(2)-O(3) bond would give rise to a decrease of the covalency of competing Na-O(3) bond. Figure 6 clearly shows this competing bond effect, where the shortening of Ti(2)-O(3) bond is always accompanied by the lengthening of competing Na-O(3) one. Thus, the increase of the sodium ion conductivity from Ln=La to Nd, Sm, Gd should not be explained on the basis of the lattice contraction but correlated to the variation of the covalency of actual Na-O bond. Such a consideration is consistent with the Brønsted acidity of $HCa_{2-x}La_xNb_{3-x}Ti_xO_{10}$ series.[13] $HCaLaNb_2TiO_{10}$ in which the protons may be attached to the NbO_6 octahedra is more acidic than $HLa_2NbTi_2O_{10}$ in which the protons are probably attached to the TiO_6 octahedra. Since the covalency of the Nb^{5+}-O bond would be higher than that of the Ti^{4+}-O one, the protons competing with the Nb^{5+}-O bond are expected to be more acidic than the protons competing with the Ti^{4+}-O one. Similar behavior is observed in many similar compounds. For instance, the protonated niobium-titanium oxides are less acidic than the protonated niobium ones but more acidic than titanium analogues.[6,20~22] Hence, in order to enhance the interlayer ionic mobility, the high covalency in the perovskite slab should be induced. A trial to increase the ionic conductivity by a substitution of the niobium for the titanium is in progress.

Conclusion

As far as the layered perovskite type structure is concerned, it must be noted that the layer spacing is not proportional to the unit cell *c*-parameter. On replacing the larger constituting ion by the smaller one, the decrease of the unit cell parameters is mainly induced by the contraction of the perovskite slab, the layer spacing being not related to such a decrease. On the contrary, the ionic character of the bond competing to the perovskite slab must be considered in terms of the covalency of the bond of the perovskite slab. This conclusion is consistent with the increasing tendancy of ionic conductivity for $Na_2Ln_2Ti_3O_{10}$ from Ln=La to Nd, Sm, and Gd. The development of fast ionic conductor adopting the layered perovskite structure in future, therefore, should be focused on the induction of the perovskite slab with high covalency.

References

1. Ruddlesden, S. N.; Popper, P. *Acta Crystallogr.* **1957**, *10*, 538.
2. Tilley, R. J. D. *J. Solid State Chem.* **1977**, *21*, 293.
3. Mohan Ram, R. A.; Ganguly, P.; Rao, C. N. R. *J. Solid State Chem.* **1987**, *70*, 82.
4. England, W. A.; Goodenough, J. B.; Wiseman, P. J. *J. Solid State Chem.* **1983**, *49*, 289.
5. Rebban, H.; Borel, M. M.; Raveau, B. *Mat. Res. Bull.* **1980**, *15*, 317.
6. Clement, P.; Marchand, R. *C. R. Acad. Sci. Paris, Ser. II* **1983**, *296*, 1161.
7. Jacobson, A. J.; Lewandowski, J. T.; Johnson, J. W. *J. Less-Common Metals* **1986**, *116*, 137.
8. Gondrand, M.; Joubert, J. C. *Rev. Chim. Miner.* **1987**, *24*, 33.
9. Gopalakrishnan, J.; Bhat, V. *Inorg. Chem.* **1987**, *26*, 4299.
10. Toda, K.; Kameo, Y.; Fujimoto, M.; Sato, M. *J. Cer. Soc. Jpn.* **1994**, *102*, 737.
11. Richard, M.; Brohan, L.; Tournoux, M. *J. Solid State Chem.* **1994**, *112*, 345.
12. Sato, M.; Kondo, Y.; Jin, T. *J. Cer. Soc. Jpn.* **1993**, *101*, 980.
13. Gopalakrishnan, J.; Uma, S.; Bhat, V. *Chem. Mater.* **1993**, *5*, 132.
14. Itoh, M.; Inaguma, Y.; Jung, W. H.; Chen, L.; Nakamura, T. *Solid State Ionics* **1994**, *70/71*, 203.
15. Inaguma, Y.; Chen, L.; Itoh, M.; Nakamura, T. *Solid State Ionics* **1994**, *70/71*, 196.
16. Izumi, F.; Murata, H.; Wtanabe, N. *J. Appl. Cryst.* **1987**, *20*, 411.
17. Young, R. A.; Wiles, D. B. *J. Appl. Cryst.* **1982**, *15*, 430.
18. Dehnicke, K. *Z. Anorg. Allg. Chem.* **1961**, *309*, 266.
19. Blasse, G.; Van den Heuvel, G. P. M. *J. Solid State Chem.* **1974**, *10*, 206.
20. Nedjar, R.; Borel, M. M.; Raveau, B. *Z. Anorg. Allg. Chem.* **1986**, *540*, 198.
21. Jacobson, A. J.; Johnson, J. W.; Lewandovski, J. T. *Mat. Res. Bull.* **1987**, *22*, 45.
22. Rebbah, H.; Borel, M. M.; Bernard, M.; Raveau, B. *Rev. Chim. Miner.* **1981**, *18*, 109.